Journal of the Earth Simulator, Volume 3, September 2005, 29 – 38

Large-scale parallel simulation of seismic wave propagation and strong ground motions for the past and future earthquakes in Japan

Takashi Furumura

Earthquake Research Institute, University of Tokyo
1-1-1 Yayoi, Bunkyo-ku, 113-0032, Japan
E-mail: furumura@eri.u-tokyo.ac.jp

(Received February 1, 2005; Revised manuscript accepted March 10, 2005)

Abstract Large-scale parallel finite-difference method (FDM) simulations of seismic wave propagation have been conducted using the Earth Simulator in order to clarify the complex seismic wavefield resulting from heterogeneities in structures and the source rupture process during the Hyogo-ken Nanbu (Kobe) earthquake (Mj 7.2; Mw 6.9) in 1995. High-resolution simulation using 240 nodes (1920 processing elements) of the Earth Simulator for seismic waves from the Kobe earthquake provided a very good reproduction of strong ground motions and a narrow zone of larger intensity (damage belt) appearing in the Awaji Island and Kobe-Hanshin region. Thus, the current simulation model is considered to be suitable for application in predicting strong ground motions for possible future earthquakes, such as the occurrence of a large earthquake in Tokyo. The Tokyo metropolitan area is located over a tectonically complicated region, in which M7 inland earthquakes and M8 plate earthquakes have frequently occurred. However, no large earthquake has occurred for the past 80 years. Simulation results for a hypothetical earthquake in Tokyo indicate that most population centers would be affected by significant ground shaking of Japan Meteorological Agency (JMA) intensity greater than 6 due to the strong amplification of ground motions in the thick sediments below Tokyo. Large earthquakes also produce strong shaking for relatively longer periods of approximately 6 to 8 s due to the resonance of seismic waves in the thick sedimentary basin. Such long-period ground motions would be most damaging to large-scale man-made structures, such as high-rise buildings, long bridges, and large oil reserve tanks, which were constructed in Tokyo after the 1923 Kanto earthquake.

Keywords: earthquake, finite-difference method, 1995 Kobe earthquake, seismic wave, strong ground motions

1. Introduction

Japan is situated in a very complicated tectonic region that involves the simultaneous subduction of the Philippine-sea Plate and the Pacific Plate beneath the Japanese islands. Large earthquakes have occurred frequently in Japan as a result of the interactions among and within these plates. Most of the densely populated areas in Japan are located in sedimentary basins, and the amplification of ground motions in the thick sediments results in strong ground shaking with long durations.

An important goal of strong-motion seismology is the prediction of strong-motion damage in future earthquake scenarios. Computer simulation of seismic wave propagation is indispensable in gaining a good understanding of complex seismic behavior resulting from heterogeneities in structures along the propagation path and the source rupture process adopted in the model.

Recent advances in high-performance computing technology, such as the Earth Simulator supercomputer, have helped to realize realistic simulation of seismic wave propagation on a regional scale, including small-scale heterogeneities in the subsurface structure and relatively higher frequencies of over 1 Hz. Through detailed comparison between the simulation results and observations from a dense, nation-wide, network that was recently installed across Japan, the accuracy of the simulation model has been steadily improved.

In the present paper, a parallel finite-difference method (FDM) simulation for seismic wave propagation is introduced, and the efficiency of the Earth Simulator for simulating strong ground motions is presented through simulation examples for the 1995 Kobe earthquake (Mw 6.9) and a hypothetical Tokyo earthquake scenario.

2. Parallel FDM Simulation of Seismic Waves

Seismic wave propagation in heterogeneous media is expressed by solving the equations of 3D motion and the constitutive relationship between stress and strain of the

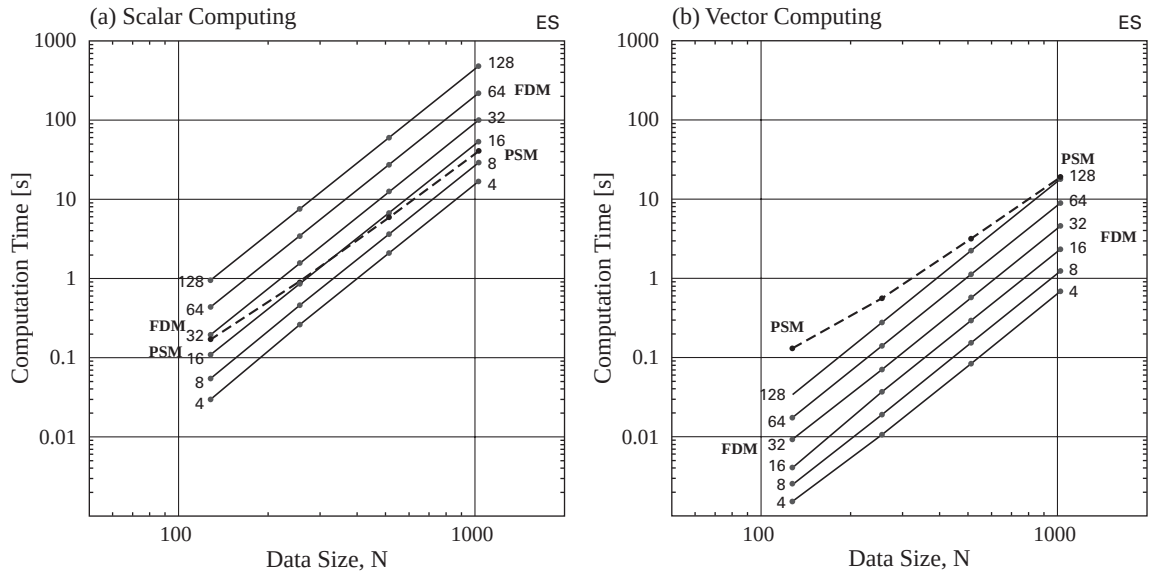

Fig. 1 Computation time for FDM (solid lines) and PSM (dashed lines) modeling (a) without using the vector hardware unit and (b) using the vector hardware unit of the Earth Simulator.

wavefield. The spatial derivatives of these equations are solved numerically using the FDM, or more accurately, by the pseudo-spectral method (PSM) using fast Fourier transform (FFT), for example.

The PSM has long been recognized as a very efficient alternative to higher-order FDMs because performing the FFT is much faster than calculating the large number of multiplications and additions required in FDM calculations. Thus, the PSM has long been used for large-scale parallel simulations of seismic wave propagations in 3D heterogeneous structures (e.g., [1, 2]).

However, the PSM has not been applied to vector computers such as the Earth Simulator, because even FFT that has been fully optimized for implementation on a supercomputer can not achieve good performance on vector hardware. Figure 1b compares the computation time for the 3D modeling of seismic waves using the PSM and higher-order FDMs on the Earth Simulator, respectively, as a function of data size and the FDM order (4, 8, 16, …, 128). In order to demonstrate the effectiveness of the vector hardware of the Earth Simulator, the same experiments were performed without using vector hardware (Fig. 1a). These figures demonstrate that the PSM is much faster than the higher-order FDMs for schemes having orders higher than 32 for scalar computing without using vector hardware (Fig. 1a). However, the advantages of the FFT over the higher-order FDMs are not as clear for vector computing on the Earth Simulator. We therefore selected higher-order FDM rather than the PSM for high-performance computation of seismic wave propagation using the Earth Simulator.

3. Parallel FDM Simulation

Parallel simulation of a 3D seismic wavefield using a large number of processors is achieved through a traditional domain decomposition approach (e.g. [3]), in which the 3D model is divided vertically into a number of subregions that are assigned to several processors. A message-passing interface (MPI) is employed for the exchange of data between neighboring nodes at each time step in order to pass the wavefield between neighboring subregions.

The Earth Simulator has a shared memory symmetric multiprocessor (SMP) cluster architecture and consists of 640 SMP nodes. Each SMP node is comprised of eight vector processors (PE). Thus, dual-level parallel programming can be applied for domain partitioning in the parallel FDM.

A single-level flat MPI model is commonly used as a programming structure for the Earth Simulator, in which separate single-threaded MPI processes are executed on each PE. An alternative approach that makes full use of the complex architecture of the Earth Simulator is a multi-level parallelization using MPI between nodes in combination with loop-level parallelism within each node, achieved through compiler-based thread parallelization (e.g., micro task, or Open MP). Figure 2 compares the performance of two parallel computing algorithms for the domain partitioning FDM simulation as a function of node numbers. Both parallel models provide similar levels of performance for a small number of nodes, but the SMP/MPI hybrid model displays somewhat better performance as the number of nodes increases. This is mainly because flat MPI requires eight times as many as partitions of the computational domain, and

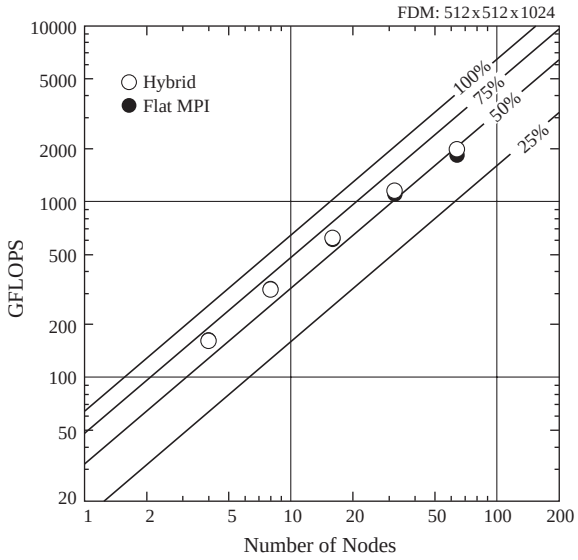

Fig. 2 Parallel performance of the Earth Simulator in GFLOPS for 3D parallel FDM simulation using 4 to 64 nodes using flat MPI (solid circle) and SMP/MPI hybrid (open circle) parallel algorithms. The diagonal lines indicate the efficiency of the parallel computing (25, 50, …, 100%) relative to peak speed.

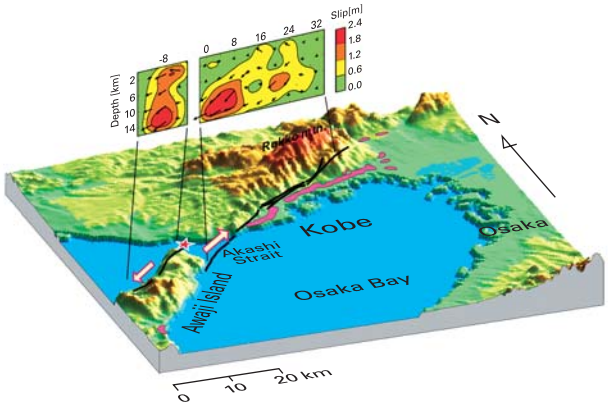

Fig. 3 Index map of the 1995 Kobe earthquake. The star symbol, black lines, and arrows indicate the epicenter, source faults and fault rupture directions, respectively. Purple zones are highly damaged areas of JMA intensity 7 (damage belt). The source slip distribution along the fault planes is projected above the raised relief map.

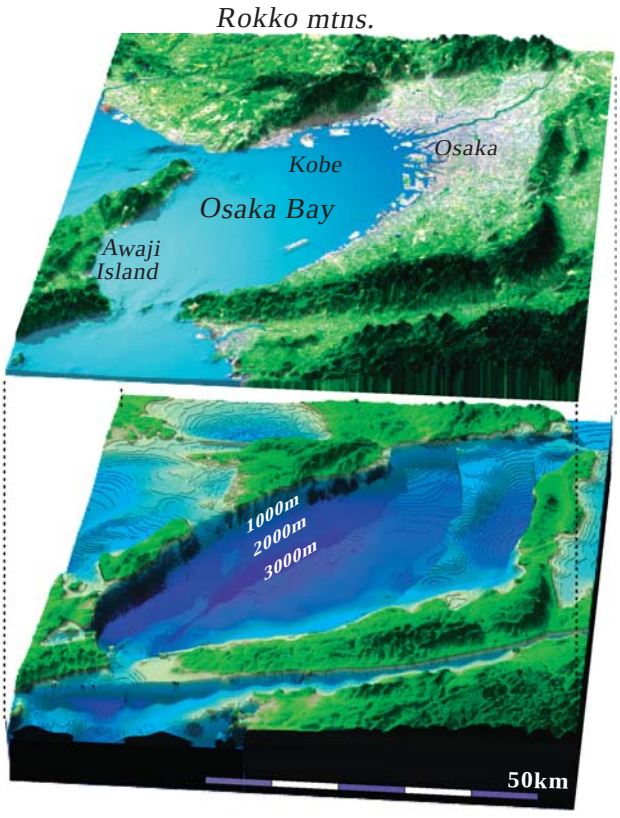

Fig. 4 Topography of Kobe-Hanshin area, and the subsurface structure of the bedrock/sediment interface.

so the overhead of MPI communication relative to the main FDM computation on each node reduces the performance of the FDM simulation. Moreover, the length of vector computing unit (vector length) at each node is considerably reduced when over partitioning occurs with a large number of processors. Thus, the SMP/MPI hybrid approach for the Earth Simulator offers much better performance compared to the flat MPI, especially using a large number of PEs. The parallel FDM simulation achieves good performance with efficiencies of 40% to 60% of the peak value for all PEs (64 GFLOPS/node).

4. Parallel Simulation of the 1995 Kobe Earthquake

The Hyogo-ken Nanbu (Kobe) earthquake of January 17, 1995 (Mw 6.9) was the most damaging in modern Japanese history, killing over 6,700 people in Kobe and the Hanshin region. A notable feature of this earthquake was that most of the damage occurred within a narrow zone, which came to be known as the “damage belt”. The damage belt extends for over 25 km crossing the city of Kobe with a width of approximately 2 km (purple zone in Fig. 3). The largest intensity (of 7) occurred inside the damage belt. Usually, fault rupture propagation produces strong ground shaking in the area above the fault, but the damage belt is displaced noticeably from the actual fault (black lines in Fig. 3) toward the center of Kobe at an offset distance of approximately 1 to 2 km, due to the bending of ray paths and multi-passing effects of seismic waves in the complex subsurface structure below Kobe.

Researchers have long attempted to simulate the strong ground motions that occurred during the Kobe earthquake. However, the patterns of the intensity distribution derived in these simulations were not clear enough to reproduce the sharp contrast of the narrow and long dam-

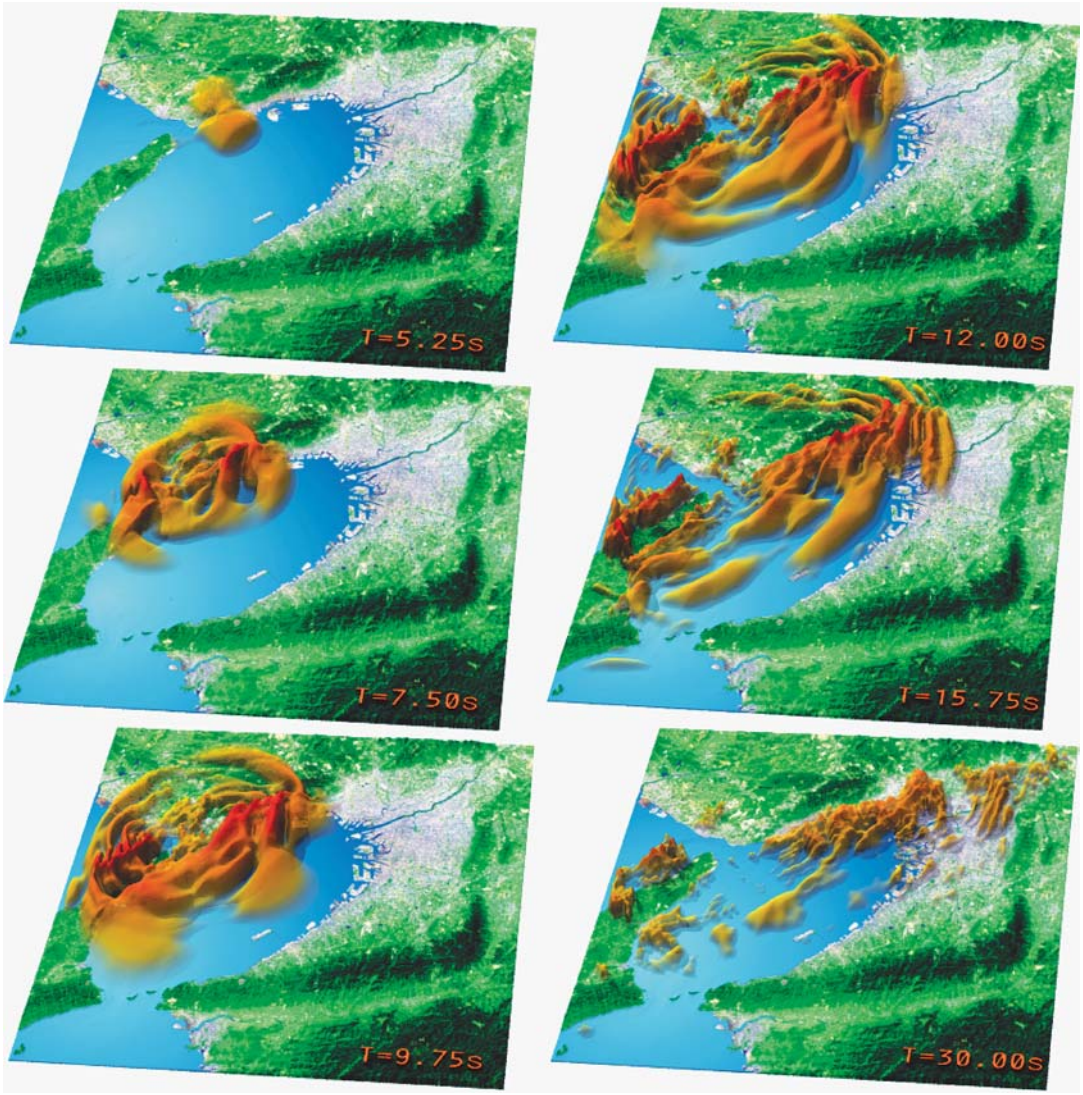

Fig. 5 Progression of seismic wave propagation of horizontal ground velocity motions derived from the simulation (The time is shown at the bottom-right corner of each frame.)

age belt (e.g., [4, 5]), due to insufficient resolution of the structural model and the high-frequency signals employed in simulations.

Ten years after the destructive Kobe earthquake, improvements in computing power have made it possible for large-scale simulation of strong ground motions with relatively higher-frequencies of over 1 Hz. In addition, a high-resolution structural model of Kobe with a resolution of 100 m in the horizontal direction and 50 m in the vertical direction has been constructed by the Geological Survey of Japan based on a large number of reflection and refraction experiments conducted in the Osaka basin ([6], Fig. 4).

4.1 Simulation Model

Therefore, we conducted a high-resolution computer simulation of seismic wave propagation using the Earth Simulator and the latest high-resolution subsurface structural model in order to try to reproduce the narrow damage belt. The present simulation model covers a zone of 90 km × 85 km × 40 km which has been discretized by a small grid spacing of 0.05 km × 0.05 km × 0.025 km (Fig. 4). The mesh size of the present simulation is four times smaller than that used in the previous experiment [4], and the target area is larger than of the previous simulation requires a 62.6 billion grid-point model. Although the scale of the present simulation is approximately 1,500 times larger than that of the previous experiment, the simulation was easily handled by the Earth Simulator.

The minimum shear wave velocity in the most shallow layer below Kobe is 0.25 km/s, and the small grid size (0.05 km) used in the model allows calculation of seismic waves of up to 2 Hz at a sampling of 2.5 grid points per shortest wavelength. The seismic source is introduced by

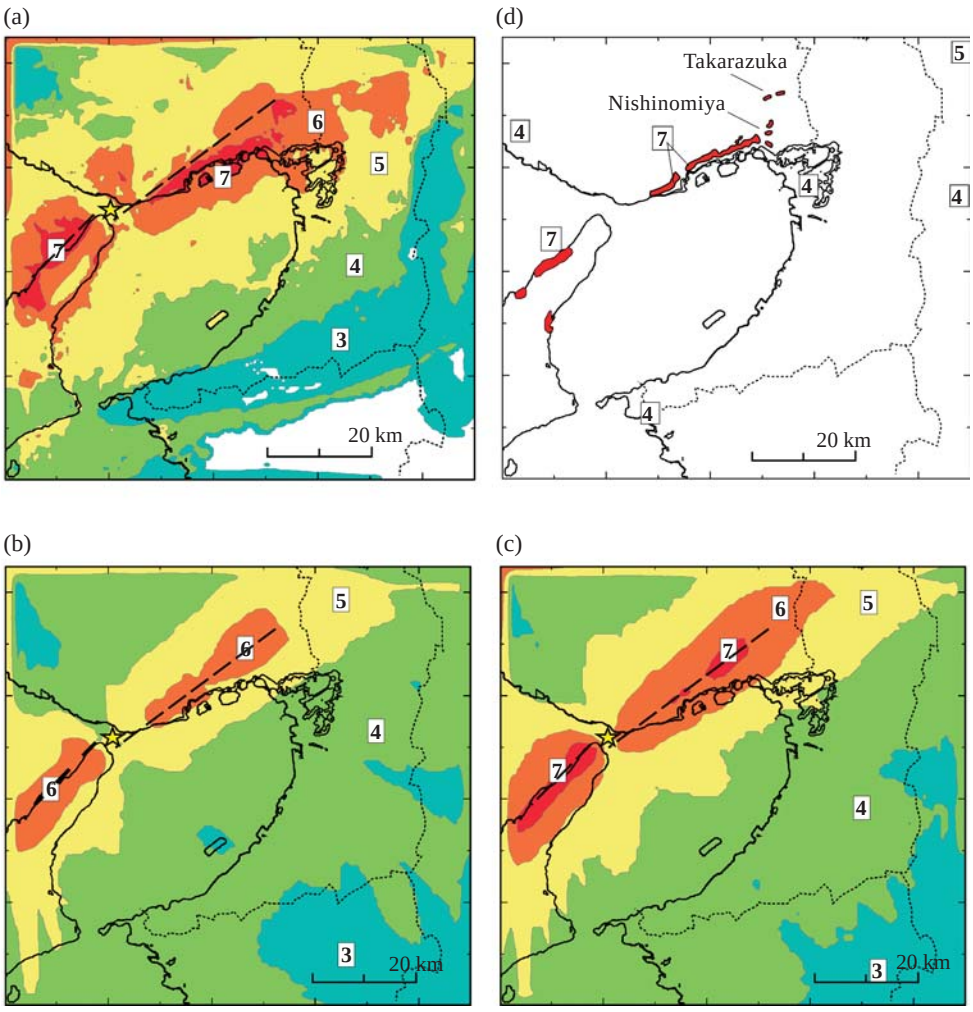

Fig. 6 Distribution of simulated JMA intensity on a seven-point scale using (a) the detailed 3D subsurface structure of the Kobe-Hanshin area, (b) the layered structure, excluding sedimentary layers over rigid bedrock, and (c) 2-km-thick sediments covering the entirety of the bedrock.(d) Observed intensity and the area of the damage belt (red zones). The star symbol and dashed lines indicate the hypocenter and the source fault, respectively.

assigning a number of double-couple point sources on the fault plane, each of which radiates seismic waves with a maximum frequency of 2 Hz. The fault rupture runs bi-laterally from the hypocenter to the northeast and southwest at an average rupture velocity of 2.5 km/s. Since the source-slip models so far derived from the inversion of strong motion waveforms and GPS data use the relatively lower frequency band below 0.5 Hz, simply applying these models for high-frequency radiations of over 0.5 Hz is not adequate. Recent studies on source-rupture process claimed that high-frequency signals are mostly controlled by the irregularities in the source rupture speed. We therefore modified the smooth slip model derived by the inversion mentioned above by introducing a random fluctuation in the fault-rupture velocity at each sub fault on the fault plane. Such heterogeneities in the fault-rupture process efficiently produce high-frequency signals in the simulated wavefield. By comparing the simulated waveform and observations, the parameter for the standard deviation of random fluctuation was finally selected as 2%.

The simulation model is surrounded by the perfect matching layer [7] of a 20-grid-point absorber in order to eliminate artificial reflections and wraparound noises occurring at boundaries. The 3D simulation uses approximately 0.74 TB of computer memory, and a CPU time of approximately three hours by parallel computing using 240 nodes (1920 PEs) of the Earth Simulator. A good vector performance of over 99.5% was achieved, and the simulation extraction reached over 40% of the peak speed.

4.2 Simulation Results

The progression of simulated ground motions of horizontal velocity motion for the Kobe earthquake is shown in Fig. 5. In the first frame (T = 5.25 s), the seismic wave

begins to appear at the surface near the Akashi Strait, and at T = 7.5 s, a directivity pulse generated from the rupturing fault is very clearly approaching Kobe. The directivity pulses propagate northeastwards in the Rokko mountain region at a relatively faster speed of approximately 3 km/s and eastwards on the Kobe side at a very low speed of less than 1 km/s (T = 9.7, 12, 15.7 s). At 9.75 s, another directivity pulse is being generated from the second large slip (asperity) on the fault at 10 km below Kobe (see, top panel of Fig. 3). These two pulses are amplified significantly in the thick, low-velocity sediments below Kobe and form longer tails in the basin. A surface wave is produced at the edge of the mountain/basin interface by the conversion of an S-wave propagating upward from the source to Rokko mountains side. The surface wave then enters the sedimentary basin, resulting in stronger ground shaking by constructive interference between the basin waves propagating upward from the source to Kobe side. These signals propagate through Kobe from west to east by multiple reflections inside the basin, which causes a large and very long ground shaking in the densely populated areas (T = 30 s).

The pattern of seismic intensity distribution derived through the present simulation is shown in Fig. 6a, where a narrow and long zone of JMA intensity 7 is clearly seen to the southeast of the fault zone. The simulation result is similar to the observations in terms of intensity-7 zones with the width of the belt (approximately 1 to 2 km), and some pockets of localized intensity-7 zones at eastern side of the main damage belt, such as those at Takarazuka and Nishinomiya. In contrast, these observations were not reproduced well in the previous simulations due to their coarse mesh model [4, 5].

The results of the simulation imply that information on the detailed structure of the shape of the basin is vitally important, and that such localized areas of larger intensity are very sensitive to the structures of the basin edge and the shallow superficial layers. In order to reinforce these findings, we conducted another set of computer simulations using simplified layered structural models for Kobe and the same source-slip model as in the first simulation. The second simulation assumes that the city of Kobe is located over rigid bedrock, so that no amplification in the sedimentary layer occurs below the city (Fig. 6b). The result is very simple. The pattern of intensity distribution is symmetric above the fault trace at relatively smaller intensities of less than 6. The third simulation examines the amplification effect of the low-velocity superficial layer covering the rigid bedrock. These results also show a symmetric pattern with maximum intensities of 7 just above the asperities on the fault plane in Kobe and on Aawji Island.

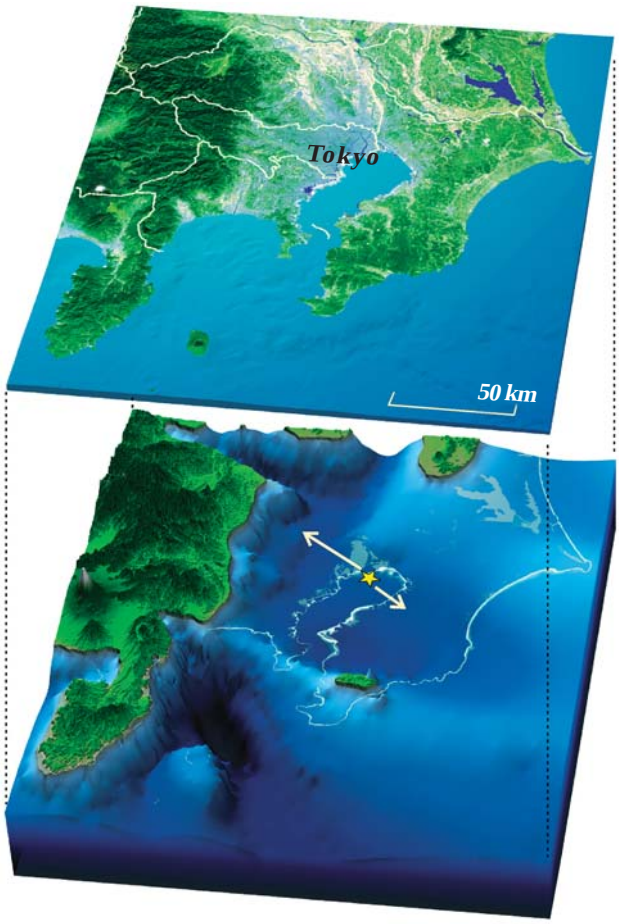

Fig. 7 Subsurface structure model of the Kanto area illustrating the topography of the sediment/basement interface. The star symbol and arrows indicate the hypocenter and the directions of fault rupture assumed in the simulation, respectively.

Both simple structural models failed to explain the discrepancy between the large intensity zones and the fault trace.

5. Estimation of Ground Motions for a Hypothetical Tokyo Earthquake Scenario

The Tokyo metropolitan area has been affected by strong motion damage from three large earthquakes: the 1923 Kanto earthquake (M7.9), the 1703 Genroku earthquake (M8.4), and the 1855 Ansei Edo (M7) earthquake. Whereas the former two seismic events occurred at the interface between the subducting Philippine-sea Plate and the North American Plate, the latter event is considered to have occurred in the north of Tokyo bay but the source mechanism and depth are unknown.

Several attempts have been made to determine the source mechanism of the Ansei Edo earthquake through analysis of the pattern of seismic intensity distribution in the area around Tokyo (e.g., [8]). However, the intensity

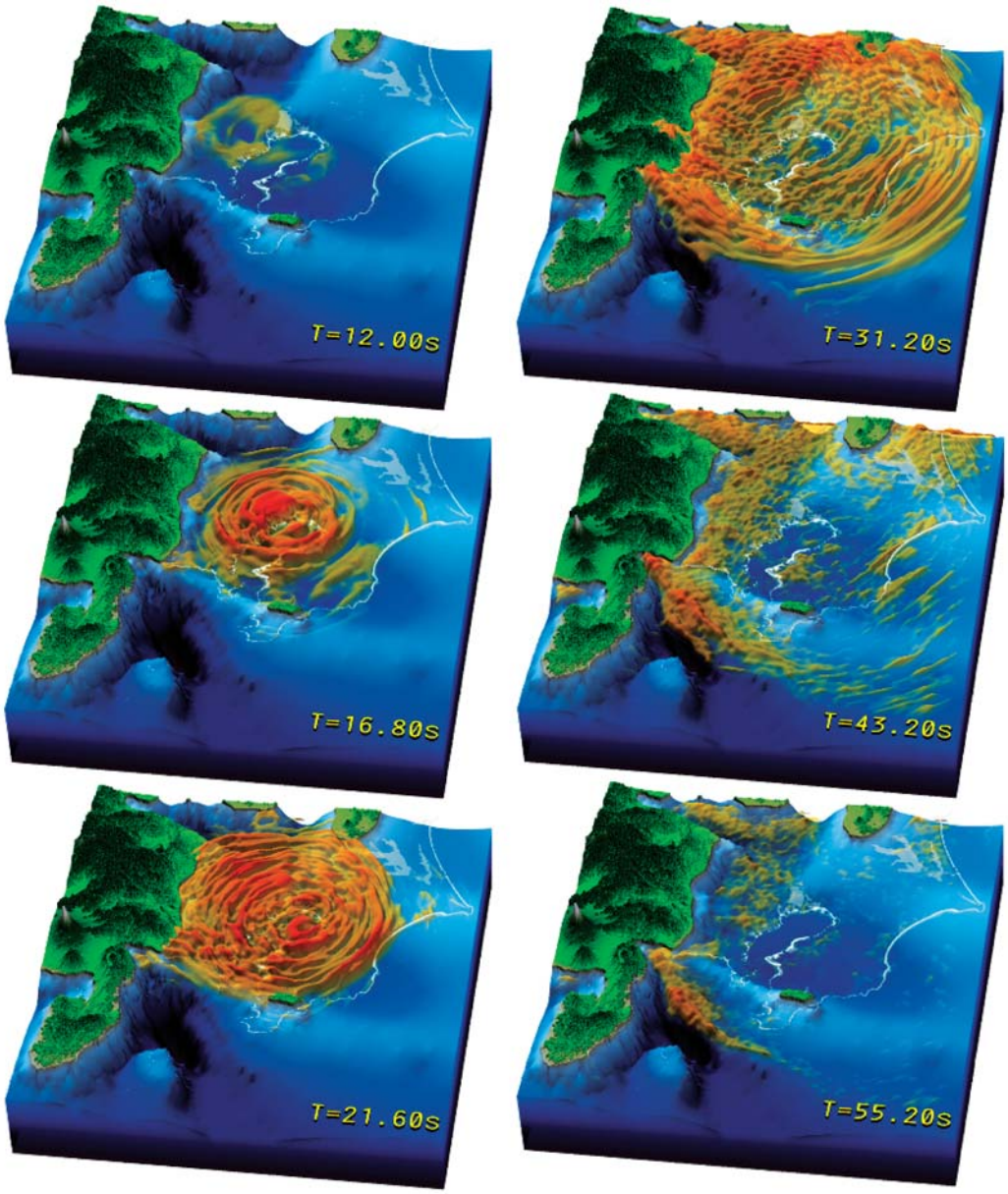

Fig. 8 Progression of simulated surface ground motions of a hypothetical Tokyo earthquake (M7.2). The time at the bottom-right corner of each frame indicates the time after fault rupture initiation.

pattern in Tokyo would be considerably affected by the amplification effect of the thick sediments, and thus estimating the source depth from the local intensity pattern in Tokyo has been proved very difficult.

Recently the authors attempted to use the intensity distribution on a regional scale to examine the possible source depth of the Ansei Edo earthquake, because large-scale anomalies of regional intensity pattern would be affected by deep and large-scale subsurface structures in the crust and upper-mantle structures rather than the localized anomalous structure beneath Tokyo ([9]). We used the Earth Simulator to simulate the regional pattern of intensity for three possible earthquakes at depths of 8, 40, and 80 km and compared these patterns with observations. As a result, the source model that properly explains the peculiar intensity pattern for the Ansei Edo earthquake was determined to be the shallow event (h = 8 km) in the crust, as was the case for the 1995 Kobe earthquake ([10]).

If such a shallow earthquake did occur north of Tokyo Bay, the Tokyo metropolitan area would potentially suffer from strong motion damage by similar earthquakes. We therefore conducted a simulation of strong ground motions caused by a shallow, crustal, earthquake if occurred in the Tokyo area.

5.1 Simulation Model

The structure of the Kanto basin has been extensively

investigated since 1980 through a number of geophysical and geological experiments, such as a reflection and refraction surveys, array measurements of micro tremors, analysis of gravity anomalies, and using deep drilling logs [11]. The basin model can be expressed by three sediment layers, having respective shear-wave velocities of 0.5 km/s, 1.0 km/s, and 1.7 km/s, overlying rigid bedrock (3.0 km/s). The maximum thickness of the sedimentary layer is approximately 4 km at the center of Tokyo bay.

The simulation model is 204 km × 204 km × 128 km, which was discretized by a grid size of 0.1 km × 0.1 km × 0.05 km in a shallow layer to a depth of 8 km, and the grid size is doubled (0.2 km × 0.2 km × 0.1 km) in the deeper layers. Such a multi-grid approach for FDM simulation can reduce the computer memory and time requirements by a dozen orders, as compared with the conventional FDM using a uniform mesh. We used the same source model as for the 1995 Kobe earthquake (Mj 7.2). The simulation assumes that the fault rupture starts at the north of Tokyo bay at a depth of 14 km, and spreads bilaterally to the northwest and southeast, similar to most of the other active faults in the vicinity of Tokyo. The simulation evaluates seismic wave propagation at a maximum frequency of 1 Hz.

5.2 Simulation Results

The results of the simulation are shown in Fig. 8 for the seismic wave propagation from T = 12 s to 55.2 s after the start of fault rupture at the hypocenter. The progression of the seismic wave propagation demonstrates the process of strong motion generation on the surface and significant amplification of the ground motion in the thick sedimentary basin. The amplification and elongation of the ground motion is noticeable in the center of Tokyo, which has a thick sediment cover (> 4,000 m). Very large and long duration of ground motions is distinct at northern and eastern edges of the basin, where the ground motion encounters a sharp wall of basement rock for propagating outside of the basin.

The pattern of the intensity distribution for the hypothetical Tokyo earthquake derived by the simulation is shown in Fig. 9, in which intensities of greater than 6 cover the high-population areas almost entirely. The simulated acceleration seismograms are multiplied by site amplification coefficients that were derived empirically from the relationship between the surface geology and the site amplification effect [12], because such amplification effects due to shallow (< 20 m) superficial layers are not able to include in the present simulation model (50 m).

Areas of larger intensities of 7 occur around Tokyo Bay and in pockets in Saitama, Ibaraki, and Kanagawa. These areas are caused by strong amplification of high-frequency signals in superficial layers, such as those extending along rivers and reclaimed land. The pattern of intensity distribution for the present Mj 7.2 earthquake simulation roughly explains that for the 1855 Ansei Edo (M7) earthquake, although the intensity of the current M7.2 simulation is roughly 1 to 1.5 points higher in intensity than the M7 earthquake.

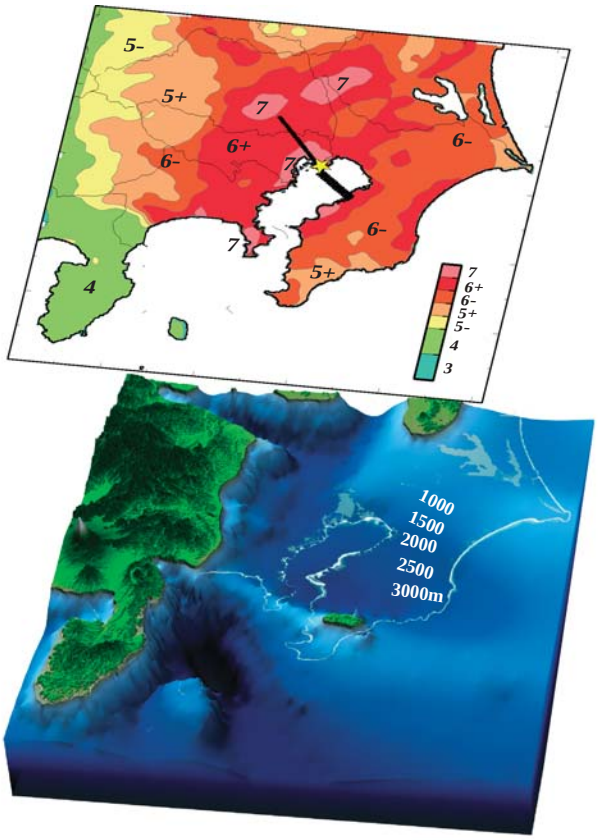

Fig. 9 Pattern of intensity distribution derived from the simulation. The star symbol and the black rectangles indicate the hypocenter and the projection of source fault, respectively. The topography of sediment/bedrock interface is shown below.

Figure 10 illustrates the simulated waveforms of horizontal ground velocity motions at Kumagaya and Shinjuku, located to the north and in the center of Tokyo, respectively. A pulsive S-wave having an amplitude greater than 100 cm/s occurs in Shinjuku, but the duration of the ground motion near the source site is rather short (less than 15 s). The dominant period of simulated ground motion is approximately 7 s. In contrast, Kumagaya is located over the edge of the basin, so the elongation of ground shaking is more dramatic (over 60 s). The propagation shown in Fig. 8 demonstrates that the long period ground shaking in Kumagaya is caused by a trapped S wave signal due to multiple S-wave reflections between the wall and basement of the trench structure of the bedrock and free surface. This results in monochromatic

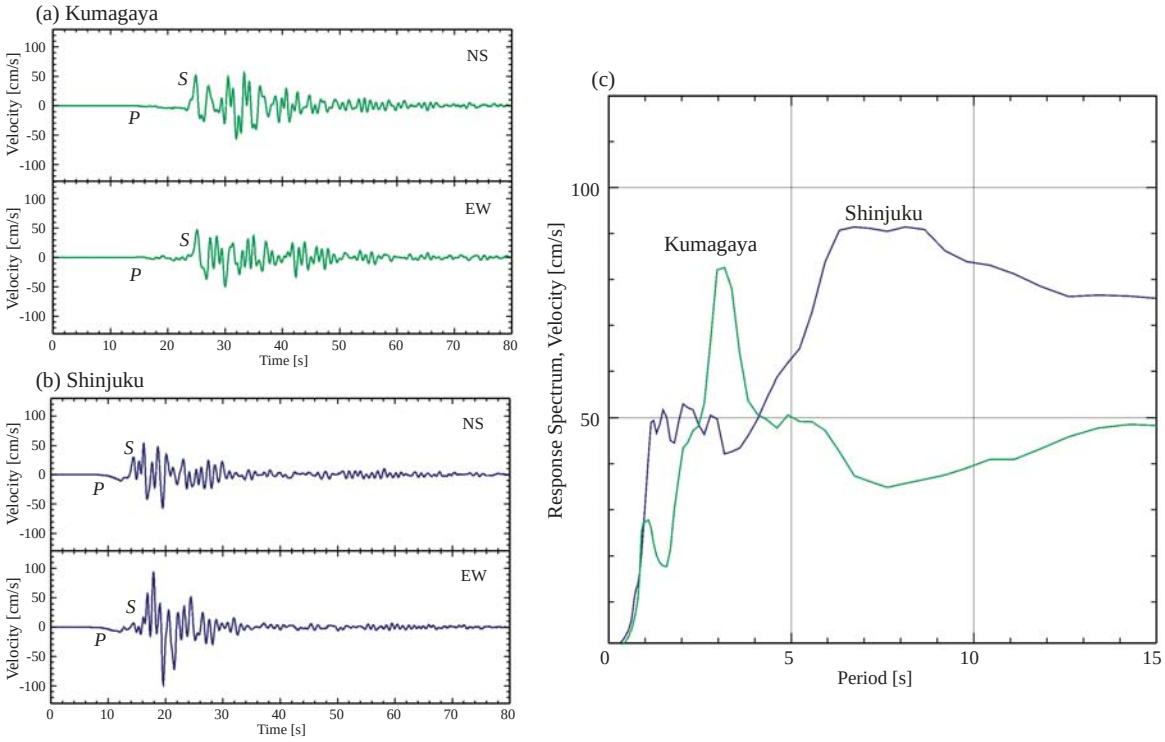

Fig. 10 Synthetic seismograms of horizontal ground velocity motions of N-S and E-W motions for the hypothetical Kanto earthquake at (a) Kumagaya and (b) Shinjuku. (c) Velocity response spectrum of horizontal ground motions for these sites (5% damping).

oscillating behavior in the waveform with a predominant period of approximately 3 s.

Potential damage to manmade structures having different resonant periods can be evaluated based on the velocity response spectrum, shown in Fig 10b. This diagram illustrates the peak amplitude of resonance for buildings having different resonant periods. A large resonance of approximately 80 cm/s occurred in Kumagaya for a resonance period of approximately 3 s, which roughly corresponds to a tall building of approximately 30 stories. Long-duration monochromatic signals may also enhance the damage to these buildings. On the other hand, longer-period ground shaking with a dominant period of approximately 7 s in Shinjuku should cause more larger shaking of over 90 cm/s to taller buildings of approximately 60 to 80 floors, which have a natural period of approximately 6 to 8 s.

6. Conclusion

As demonstrated by the 1995 Kobe earthquake, the generation of strong ground motions, and the consequent damage, are strongly affected by the interaction between the heterogeneous subsurface structure and the complex source rupture history. Therefore, the prediction of strong ground motions for future events requires a good understanding of the seismic wavefield resulting from such heterogeneities by analyzing observed waveforms by dense seismic array and corresponding computer simulations.

Recent accomplishments at high-performance computing facilities such as the Earth Simulator have made it possible to conduct realistic simulation of seismic wave propagation on a regional scale for relatively higher frequencies of over 1 Hz. In the present study, the generation process of strong motion damage in the 3D basin structure during the 1995 Kobe earthquake has been clearly demonstrated by a large-scale FDM simulation using a high-resolution subsurface structural model of Kobe. A good match between simulated and observed intensity patterns during the earthquake demonstrates the effectiveness of computer simulation for accurate reproduction of seismic wave propagation for the possible future earthquake scenarios, such as the large earthquake anticipated to occur in Tokyo.

Acknowledgements

Support for the present study was provided under a joint research project in cooperation with the Earth Simulator Center entitled “Numerical simulation of seismic wave propagation and strong ground motion in 3D heterogeneous media”. Additional support was provided under the Special Project for Earthquake Disaster Mitigation in Urban Areas from the Ministry of

Education, Culture, Sports, Science and Technology of Japan. The grid data of a 3D subsurface structure model of the Osaka basin was provided by a CD-ROM published by Geological Survey of Japan. The author appreciates the careful and thoughtful review and comments by Prof. T. Yukutake.

(This article is reviewed by Dr. Takesi Yukutake.)

Reference

[1] M. Reshef, D. Kosloff, M. Edwards and C. Hsiung, Three dimensional acoustic modeling by the Fourier method, *Geophysics*, vol.**53**, pp.1175–1183, 1998.

[2] T. Furumura, B.L.N. Kennett, and H. Takenaka, Parallel 3-D pseudospectral simulation of seismic wave propagation, *Geophysics*, vol.**63**, pp.279–288, 1998.

[3] T. Furumura, K. Koketsu, and K.-L. Wen, Parallel PSM/FDM hybrid simulation of ground motions from the 1999 Chi-Chi, Taiwan, earthquake, *Pure and Applied Geophysics*, vol.**159**, pp.21330–2146, 2002.

[4] T. Furumura, and K. Koketsu, Specific distribution of ground motion during the 1995 Kobe earthquake and its generation mechanism, *Geophys. Res. Lett.*, vol.**25**, pp.785–787.

[5] A. Pitarka, K. Irikura, T. Iwata, and H. Sekiguchi, Three-dimensional simulation of the near-fault ground motions for the 1995 Hyogo-ken Nanbu (Kobe), Japan, earthquake, *Bull. Seism. Soc. Am.*, vol.**88**, pp.428–440, 1998.

[6] H. Horilawa, K. Mizuno, T. Ishiyama, K. Sateke, H. Sekiguchi, Y. Kase, Y. Sugiyama, H. Yokota, N. Suehiro, T. Yokokura, Y. Iwabuchi, N. Kitada, and A. Pitarka, A three-dimensional subsurface structure model beneath the Osaka sedimentary basin, southwest Japan, with fault-related structural discontinuities, Katsudansou-Kojishin Kenkyu Hhoukoku, vol.**3**., pp.225–259, 2003.

[7] C. Marcinkovich, and K. Olsen, On the implementation of perfectly matched layers in a three-dimensional fourth-order velocity stress finite difference scheme, *J. Geophys. Res*, vol.**108**, doi:1029/2002JB002235, 2003.

[8] T. Hikita and K. Kudo, Estimation of source parameters and strong ground motions during the 1855 Ansei-Edo earthquake by the empirical Green function method, *J. Struct. Eng. AIJ*, vol.**546**, pp.63–70, 2001.

[9] T. Furumura, Seismic intensity distribution and source model of the 1855 Ansei Edo earthquake: examination by numerical simulation, Abst. The Seismol. Soc. Japan, 2003 Fall Meeting, B052, 2003.

[10] T. Furumura and L. Chen, Parallel simulation of strong ground motions during recent and historical damaging earthquakes in Tokyo, Japan, Parallel Computing, 2005, in press.

[11] H. Yamanaka and N. Yamada, Estimation of 3D S-wave velocity model of deep sedimentary layers in Kanto plain, Japan, using microtremor array measurements, *Butsuri-Tansa*, vol.**55**, pp.53–65, 2002.

[12] T. Kubo, Y. Hisda, A. Shibayama, M. Ooi, M. Ishida, H. Fujiwara, and K. Nakayama, Development of digital maps of site amplification factors in Japan, and their applications to early strong motion estimations, *Zisin*, vol.**56**, pp.21–37, 2003.